Conductance of Dilute LiCl, NaCl, NaBr, and CsBr Solutions in Supercritical Water Using a Flow Conductance Cell

Miroslaw S. Gruszkiewicz[†]

Oak Ridge National Laboratory, Chemical and Analytical Sciences Division, P.O. Box 2008, Oak Ridge, Tennessee 37831-6110

Robert H. Wood*[,‡]

Department of Chemistry and Biochemistry and Center for Molecular and Engineering Thermodynamics, University of Delaware, Newark, Delaware 19716

Received: January 13, 1997; In Final Form: June 3, 1997[⊗]

Conductivities of LiCl(aq), NaCl(aq), NaBr(aq), and CsBr(aq) solutions have been measured in the range of concentrations from 0.013 to 4×10^{-8} mol·dm^{-3} using a flow conductance cell at temperatures between 603 K and 674 K and pressures between 15 MPa and 28 MPa (water densities from 650 to 200 kg·m^{-3}). Limiting equivalent conductances and ionization equilibrium constants calculated from the concentration dependence of the equivalent conductance are reported. Previous measurements of equilibrium constants in the low-density supercritical region, although of lesser accuracy, agree well with the present results. Even at the critical density and 2.5 K above the critical temperature there is no evidence for the critical effects which make the Debye−Hückel limiting law invalid at the critical isotherm−isobar. No critical scaling of Λ_0 is observed. Walden's rule is not obeyed and the Stokes radius increases by 70% near the critical region as the density goes from 700 to 200 kg·m^{-3}, suggesting an increase in the number of water molecules carried along with the ion. The differences in mobility between different ions are rather small when compared to the differences in crystallographic ionic radii. The association constants are in the order CsBr < NaBr < NaCl $\approx$ LiCl.

I. Introduction

A new high-temperature flow conductance apparatus with significant improvements in speed and accuracy has been recently built at the University of Delaware. Construction details, as well as conductance results for NaCl(aq), LiCl(aq), NaBr(aq), and CsBr(aq) at high temperatures, have been described.[1] These measurements were made relatively far from the critical point of water, mostly on the 28 MPa isobar, with a few measurements taken at lower pressures, but at temperatures well below the critical point. Shown in Figure 1 is a phase diagram of water with symbols representing the conditions where the conductance of NaCl(aq) was measured. For a long time the only conductance measurements for electrolytes in the region adjacent to the critical point of water (understood here as the area in the temperature range 645−660 K and in the density range 240−400 kg·m^{-3}) were the pioneering investigations of Fogo *et al.*[2] followed with an extension to higher densities by Pearson *et al.*[3] Lukashov *et al.*[4] made measurements at the saturation curve in the density range from 700 to 85 kg·m^{-3} and reported the resulting equivalent conductances at infinite dilution together with ionization equilibrium constants, but unfortunately did not report experimental data. The measurements of Martynova *at al.*[5] only go to 500 kg·m^{-3} on the saturation curve. Recently, the apparatus[6] used previously by Marshall and co-workers for investigations to very high temperatures was modified by Ho *et al.*[7] and used for measurements including the region close to the critical point of water (see Figure 1). This region is interesting, because some phenomena important for understanding both natural (geological) and industrial processes (ion hydration and ion pairing as well as chemical reaction equilibria and kinetics) should be influenced by the closeness of the critical region. Generally, because of the significant difficulties associated with measurements at high temperature in low-density water, there are not enough data available for low-density steam solutions, which are important to the electric power generation industry.

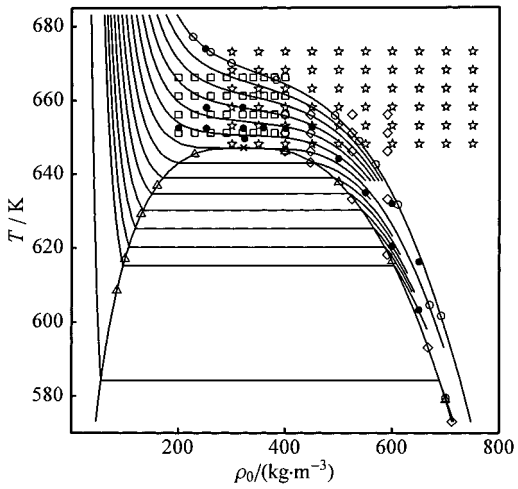

Figure 1. Phase diagram of water with state conditions where conductance measurements for NaCl(aq) were made. The isobars are 10 MPa and 15, 16, ..., 28 MPa. The symbols represent the measurements of, (□) Fogo *et al.*;[2] (◇) Pearson *et al.*;[3] (☆) Ho *et al.*;[7] (○) Zimmerman *et al.*[1]; (△) Lukashov *et al.*;[4] (●) this work. The critical point is marked by ×.

It should be expected that extrapolation toward the critical point of simple empirical correlations of the ion pair dissociation constants and limiting conductances as functions of temperature

* To whom correspondence should be sent.
† xuk@ornl.gov.
‡ rwood@udel.edu.
⊗ Abstract published in *Advance ACS Abstracts,* July 15, 1997.

S1089-5647(97)00197-1 CCC: $14.00 © 1997 American Chemical Society

and density, determined from measurements far from the critical point of water, will fail as the critical point is approached. Indeed, the results of Fogo *et al.*[2] showed a significant change of slope in the temperature dependence of K_m occurring already relatively far from the critical region. One of the goals of this work was to explore K_m and Λ_0 near the critical point. In this paper we present an extension of the previous results on the same solutes to the region closer to the liquid−vapor equilibrium envelope, including the region close to the critical locus of the solutions. Conductivities were measured at temperatures between 603 and 674 K and pressures between 15 and 28 MPa. Water densities corresponding to these conditions were between 650 and 200 kg·m^{-3}. The new measurements confirmed the greater precision and extended temperature and concentration ranges available for investigation with the new instrument. The very strong ion pairing at low water densities makes it necessary to make measurements at very low concentrations in order to obtain reliable limiting equivalent conductances. To get as close as possible to the Onsager limiting law region, measurements were made at concentrations as low as 4×10^{-8} mol·dm^{-3}. It was also desirable to extend the measurements as close as possible to the critical point to obtain information about critical behavior. Conductance of NaCl(aq) was measured at the critical water density and 2.5 K above the critical temperature of water. This distance from the critical point is close to the limit of our method for obtaining the ionization constants, since the temperature of the critical point of a 0.01m NaCl solution is 2.2 K above the critical temperature of pure water. Obtaining equilibrium constants any closer to the critical point would require narrowing the concentration range in which conductances are measured in order to stay away from the two-phase region. This would impose even higher requirement on accuracy, and this is hard to achieve using a flow instrument with a highly compressible supercritical fluid.

The accuracy of the present measurements decreases at lowest densities, because of the very high impedances of the cell. High impedances can only be measured at the cost of decreased accuracy as they become commensurate with the impedance to the ground, the insulation impedance, and the impedance of parasitic capacitances. Thus, the low-density limit of the instrument was determined by the conductance cell constant, and it can be pushed to lower steam densities in the future by using a cell with a smaller constant.

II. Experimental Section

The experimental apparatus and procedure were the same as described previously.[1] One minor modification was necessitated by the failure of the cell at the highest temperature of the previous runs (673 K). This failure was caused by a shunt across the electrodes created by a layer of copper oxide formed on the sapphire insulator surface and originating from a copper washer used to protect the sapphire from cracking under uneven stress. The problem was eliminated by replacing the copper washer with one made of annealed alumina insulating tape. Another modification was adding two high-accuracy resistance decades ($10 \times 0.1\ \Omega$ and $10 \times 100\ k\Omega$) to our resistance standard. This eliminated the need for using less accurate and more time consuming methods for measuring very large and very small resistances.

After platinization of the electrode surfaces and reassembling the cell, the cell constant was determined by three approaches: first using KCl solutions at about 298 K and at ambient pressure, then with the same salt at 298 K and at 25 MPa, and finally using NaCl solutions at 298 K at ambient pressure. The FHFP equation coefficients used to correlate conductance data were taken from Justice[8] and Barthel *et al.*[9] for KCl(aq), from Fisher and Fox[10] for KCl(aq) at 25 MPa, and from Zimmerman[11] (based on results from Chiu and Fuoss,[12] Gunning and Gordon,[13] and Shedlovsky *et al.*[14]) for NaCl(aq). Both stock solutions were prepared by weight from monocrystals of the salts (dried overnight at 200 °C) using distilled and deionized water. The measurements were made at two molalities, 0.0002−0.0008 and 0.0011−0.0018 mol·kg^{-1}, and each solution was measured twice. The cell constant determined using KCl(aq) at standard conditions was 0.2127 cm^{-1}. The high-pressure result was lower by 0.02%, and the NaCl(aq) result was higher by 0.04%. These differences being equal to or smaller than the random error of our procedures, and taking into account the cell constant determinations made earlier,[1] we concluded that the cell constant was independent of pressure and concentration and known with an accuracy better than 0.05%. No errors due to polarization or Parker effect were found.

The cell constant was determined again after several months, when the present series of measurements was completed, using KCl(aq) at standard conditions. The result was lower by 1.5% than the value found before the measurements. Similar changes in cell constant were found previously.[1] They are likely to be caused by small changes of the cell dimensions with time (for example as a result of a compression of the gold seals and/or other parts of the cell due to annealing at high temperature). The cell constant measured directly before the experiments was used for calculations. As we noted before,[1] although the changes in the cell constant influence directly the conductance results, the equilibrium constants K_m, which are inferred from the change of the equivalent conductance Λ with concentration, are not significantly affected, provided that the cell constant does not change during a run which typically lasts 8 h. The changes of Λ_0 and pK_m corresponding to a ± 0.004 cm^{-1} (1.88%) change in the cell constant were calculated. As expected, Λ_0 was directly proportional to the cell constant. The change in pK_m was less than 0.01 at a water density $\rho_0 = 650$ kg·m^{-3} (p$K_m = 1.22$) and less than 0.0002 at $\rho_0 = 200$ kg·m^{-3} (pK_m =5.03). It can be then concluded that slow shifts of the cell constant over several month periods cause errors in pK_m that are smaller than the other errors. However, it can be expected that if measurements at significantly higher densities, where less ion pairing occurs, were to be made, this error in pK_m would eventually become significant.

There was a concern that the large heat capacity of water in the region close to the critical locus makes it difficult to equilibrate the incoming solution to the cell temperature. The preheaters have to work with a relatively small temperature difference, so that large temperature gradients inside the thermostat are avoided. Also, overheating the solution leading to a two-phase fluid must be avoided because it can cause major temperature disturbances due to large fluid enthalpy changes. Inadequate preheating of the solution could cause a difference between the temperature of the solution and the temperature of the stainless steel casing of the conductance cell, where the platinum resistance thermometer is located. If temperature equilibration is incomplete, it should be possible to detect a difference in the results when the flow rate of the solution is changed. A test was carried out at $T = 652$ K and $\rho_0 = 320$ kg·m^{-3}, where the flow rate was changed between 0.25 and 0.5 cm^3·min^{-1}. The differences in the measured conductances were smaller than the random experimental error, indicating that the solution flowing through the cell was sufficiently close to the thermal equilibrium with the cell body.

TABLE 1: Solvent-Specific Conductances χ_s Measured before Each of the Series of Measurements from Table 2

			χ_s (μS·cm^{-1})			
T^a (K)	p (MPa)	ρ_0 (kg·m^{-3})	NaCl	LiCl	NaBr	CsBr
603.3	15.17	650	1.974	1.913	1.952	1.963
616.2	26.01	650	2.199			2.148
620.4	17.97	600	1.326			1.301
631.9	26.01	600	1.430			1.408
634.9	21.13	550	0.883			
644.1	22.71	500	0.568			0.506
652.7	24.80	450	0.392	0.347	0.311	0.369
652.4	23.85	400	0.197			0.210
652.6	23.66	359	0.147			0.146
649.6	22.72	324	0.089			
652.5	23.50	322	0.081	0.067	0.078	0.072
658.1	25.04	322	0.075			0.098
652.5	23.25	251	0.047			0.044
658.1	24.49	251	0.028	0.029	0.032	0.028
674.0	27.97	250	0.046			0.038
652.5	22.75	200	0.021			0.016

[a] The temperature scale is the International Practical Temperature Scale of 1968.

III. Results and Data Treatment

One of the advantages of the flow method is its ability to obtain background corrections for solvent conductance by measuring the impedance of the cell filled with a portion of the same batch of conductivity water which is going to be used for the solutions. The conductivities of this water, measured before each series of measurements, are given in Table 1. The accuracy of the solvent conductivities was severely affected by the ground and insulation impedances and it deteriorated as the density of water decreased. At the lowest water densities estimated uncertainty in the solvent conductivity was 20%.

The treatment of the experimental conductance results in order to find the limiting conductances, Λ_0, and the thermodynamic equilibrium constants for the ion dissociation reaction, K_m, was essentially similar to that described earlier.[1] However, we felt that the estimates of the solution densities necessary for calculating molar concentrations, c, needed a better basis than the simple linear correlation between the solution density, ρ, and the molality, m

$$\rho = \rho_0 + Bm \tag{1}$$

used previously. In eq 1 ρ_0 is the density of water at the same temperature and pressure and B is an empirical parameter. Since the highest molalities used in this investigation were less than 0.02 mol·kg^{-1}, the densities of a large majority of the solutions were so close to the density of water that even using the density of water would not cause significant errors. However, for several measurements at temperatures and pressures close to the critical region, one or two of the most concentrated solutions could have densities significantly higher than the density of water, and in these cases the errors in $-\log K_m$ introduced by using water densities instead of the solution densities were estimated to approach at most +0.03 (a rather small change toward more ion association). The parameters B in eq 1, found from experimental volumetric data of Majer *et al.*,[15−21] depended on density, temperature, and the solute. It was difficult to estimate B at the conditions where experimental densities were not available. Additional problems are that B diverges to infinity at the critical point and that the constant value of B ignores the Debye−Hückel limiting law and the changing ion pairing, making this method unreliable very close to the critical point.

In order to estimate the apparent molar volume V_ϕ more accurately, the equation

$$V_\phi = \alpha V_{i0}^\infty - (1-\alpha)\Delta V^\infty + \frac{A_V}{1.2}\alpha \ln(1 + 1.2\sqrt{\alpha m}) \tag{2}$$

was used, where V_{i0}^∞ is the partial molar volume at infinite dilution, ΔV^∞ is the change in volume on dissociation of the ions, I is the degree of dissociation, and A_V is the Debye−Hückel limiting slope for volume. The last term in eq 2 is a truncated expression for excess Gibbs free energy obtained from the Pitzer model[22] with the two ion interaction contribution, $2RTB_V\alpha^2 m$, omitted. Using the present results for NaCl(aq) and the values of the parameter B_V calculated by Majer and Wood[21] and correlated with density by us, the ratio of this term to the total apparent molar volume, $2RTB_V\alpha^2 m/V_\phi$, was estimated. This ratio was the largest at the highest molality of each series of measurements, and decreased rapidly with decreasing molality. It reached its maximum of less than 0.02 for the measurement at $T = 674$ K, $\rho_0 = 250$ kg·m^{-3}, and $m = 0.009\,46$ mol·kg^{-1}. For most of the measurements it was less than 0.01. A 2% error in V_ϕ would introduce a much smaller error in the density of the solutions, and the error it would cause in the equilibrium constant results would be many orders of magnitude smaller then the experimental error.

The standard change in volume for the ionization reaction, ΔV^∞ in eq 2, was obtained from the thermodynamic identity

$$\Delta V^\infty = (\partial \Delta G_m^\infty/\partial p)_T = -RT(\partial \ln K_m/\partial p)_T \tag{3}$$

written for the standard molar change in Gibbs function for the ionization reaction, ΔG_m^∞, and the associated equilibrium constant, K_m, which refers to the ionization reaction written such that it does not include water as a reactant:

$$\mathrm{MA(aq)} = \mathrm{M^+(aq)} + \mathrm{A^-(aq)} \tag{4}$$

The subscript m denotes that molality is used as the measure of composition and the standard reference composition is $m^\circ = 1$ mol·kg^{-1}. After inserting the definition of the isothermal compressibility of water, κ_T, into (3), the relation between the logarithm of the equilibrium constant and the standard molar change in volume is given as

$$\Delta V^\infty = \ln 10 \kappa_T \rho_0 RT \left(\frac{\partial(-\log K_m)}{\partial \rho_0}\right)_T \tag{5}$$

Using the equilibrium constants obtained in this work to calculate ΔV^∞ is in principle an iterative process, but since the sensitivity of K_m used to calculate it is small, the corrections are insignificant after the second cycle.

The last quantity needed to calculate the apparent molar volume from eq 2, the partial molar volume of the free ions at infinite dilution, V_{i0}^∞, was taken from the values calculated by Majer and Wood[21] for NaCl for a number of temperatures and pressures. To find the values of V_{i0}^∞ at any conditions we took advantage of the observation that the generalized Krichevskii parameter $A_{12}^\infty = V_{i0}^\infty/(RT\kappa_T\rho_0)$ is a strong function of density but not temperature and pressure near the critical point.[23] Using this fact, values of $V_{i0}^\infty/RT\kappa_T^-$ from Majer and Wood[21] were fitted to an empirical function of density, so that an estimate of V_{i0}^∞ at any (T, p) conditions could be calculated.

The final equation for A_{12}^∞ was

$$A_{12}^\infty \rho_0 = a_1\left[\left(\frac{\rho_0}{a_2}\right)^7 - \left(\frac{\rho_0}{a_2}\right)^6 + a_3\right] \tag{6}$$

with $a_1 = 285\,41.7$ kg·m^{-3}, $a_2 = 790.3388$ kg·m^{-3}, and $a_3 =$

−1870.5079. The volumes of the ion pairs, $V_{ip}^{\infty} = V_{i0}^{\infty} - \Delta V^{\infty}$, were then found to obey the following correlation,

$$V_{ip}^{\infty} = -2100 \frac{\text{kg}}{\text{m}^3} \frac{RT\kappa_T}{\rho_0} \tag{7}$$

which results from eqs 5 (using the present experimental values of K_m) and 6. An equation similar to eq 7 (without the explicit dependence on the solvent density, ρ_0) was derived by Marshall[25] to calculate ΔV^{∞}. Correlation 7 indicates that $V_{ip}^{\infty}$is, as expected, negative in the region investigated, and it follows the behavior of the isothermal compressibility in the region close to the critical point. Compared to V_{ip}^{∞} obtained by Majer and Wood,[21] eq 7 gives values more negative by about 67 $\text{cm}^3\cdot\text{mol}^{-1}$ when $\rho_0 > 650$ $\text{kg}\cdot\text{m}^{-3}$, and more negative by about 20−100% as the density decreases. It should be noted that Majer and Wood determined their ΔV^{∞} from conductance data available to them in the same way as in this work, but their correlation $K_m = K_m(T,\rho_0)$ was different from the one used in the present work (eq 12).

The concentration dependence of the equivalent conductance was expressed by the FHFP (Fuoss−Hsia−Fernández-Prini) equation

$$\Lambda = \alpha(\Lambda_0 - Sc^{1/2}\alpha^{1/2} + E\, c\alpha \ln(c\alpha) + J_1 c\alpha + J_2 c^{3/2}\alpha^{3/2}) \tag{8}$$

where S, E, and J_1 were calculated following the equations given by Fernández-Prini,[25] with viscosities from Watson *et al.*,[26] dielectric constants from Archer and Wang,[27] and other water properties from Hill.[28] The degree of dissociation α in eq 8 was calculated from the mass action equation

$$K_c = \rho_0 K_m = \frac{\alpha^2 c \gamma_{\pm}^{\ 2}}{1-\alpha} \tag{9}$$

with the mean activity coefficient of the free ions, $\gamma_{\pm}$, calculated from the Debye−Hhckel limiting law

$$\gamma_{\pm} = \exp\left(-\frac{\kappa q_B \alpha^{1/2}}{1 + \kappa a \alpha^{1/2}}\right) \tag{10}$$

where κ is the reciprocal radius of the ionic atmosphere, and the parameter a was set equal to the Bjerrum distance q_B, after Justice.[8] The concentration, c, in eqs 8 and 9 was calculated from

$$c = 1/\left[V\phi + \frac{1}{\rho_0 m}\right] \tag{11}$$

with apparent molar volumes, V_ϕ, calculated from eq 2. The apparent molar volumes of all the solutions were assumed to be equal to that of NaCl(aq) at the same molality. This is not exact, but the additional error in K_m introduced by this assumption is not expected to exceed the error caused by the uncertainty in V_ϕ of NaCl(aq) itself, as calculated from eq 2.

Three parameters, Λ_0, K_m, and J_2, were found by nonlinear least-squares fitting of the above equations to the sets of (Λ, m) pairs obtained at each temperature and pressure conditions. There were at least seven such pairs available for each fit. The experimental results are listed in Table 2, together with the concentrations and the deviations of the calculated equivalent conductances from their corresponding experimental values. As before,[1] J_2 was treated as a fitting parameter, although its theoretical value could be calculated from the FHFP model. This was done in the interest of obtaining the best estimates of the other two parameters (Λ_0 and K_m) in the region where ion pairing was considerable. As water density decreases, the optimal values of J_2 become considerably different from its calculated values and they have a large uncertainty. Table 3 shows Λ_0, K_m, $-\log K_m$, and J_2 obtained from least-squares fitting along with the standard deviations of the fits.

IV. Discussion

Examples of experimental conductance results as a function of concentration are shown in Figure 2 together with corresponding fits to eqs 8−11 and the Debye−Hückel−Onsager limiting law slopes. Figure 2 illustrates that at low solvent densities ion pairing occurs at very low concentrations, so measuring conductances as close as possible to this region helps in obtaining reliable extrapolations to infinite dilution and accurate equilibrium constants. The lowest concentration measured at $\rho_0 = 250$ $\text{kg}\cdot\text{m}^{-3}$ and $T = 674$ K was 5×10^{-7} $\text{mol}\cdot\text{dm}^{-3}$. Figure 2 shows that even near the critical density of water and only 2.5 K above the critical temperature (649.59 K and 323.7 $\text{kg}\cdot\text{m}^{-3}$) there is no evidence for problems in fitting the data with eqs 8−11. This is rather surprising, since Chang and Levelt-Sengers[29] have shown that on the critical isotherm-isobar the Debye−Hückel limiting law (eq 10) is overwhelmed by a critical scaling law, and $\ln \gamma_{\pm} = cx^{1/\delta} + ...$ with $\delta \approx 4.7$. Close to the critical isotherm−isobar a vestige of this behavior is expected. It seems unlikely that significant deviations from the Debye−Hückel limiting law (10%) would allow eqs 8−11 to fit the data within experimental uncertainty.

Walden's rule states that the product of limiting equivalent conductance and viscosity is independent of temperature and pressure, and this rule is quite accurately obeyed for a wide variety of ions in aqueous and nonaqueous solvents near room temperature. The rule is based on a continuum model of conductance and should be exact for very large ions. One of the surprising things about limiting electrical conductivities in supercritical water is that Walden's rule is not obeyed, as Marshall and co-workers[30−32] have shown in their series of publications exploring conductance in supercritical aqueous solutions. The present results allow us to look at the Walden product $\Lambda_0\eta$ near the critical point of water. Figure 3a shows a three-dimensional plot of $\Lambda_0\eta$ versus temperature and density for the present results together with the earlier results of Zimmerman *et al.*[1] This plot shows that $\Lambda_0\eta$ drops by 70% near the critical region as the density goes from 700 to 200 $\text{kg}\cdot\text{m}^{-3}$. Interestingly, Quist *et al.*[30] noted a similar drop of the Walden product with decreasing density for K_2SO_4 solutions below $\rho_0 = 500$ $\text{kg}\cdot\text{m}^{-3}$ at temperatures from 673 to 1073 K, but they attributed this behavior to unreliable extrapolations of their conductances Λ to infinite dilution. This explanation seems to be plausible, if the lowest molality investigated by Quist *et al.*[30] ($m^{0.5} > 0.02$ $\text{mol}\cdot\text{kg}^{-1}$) is positioned on the abscissa in Figure 2 in order to visualize the length of the extrapolation involved. It is also noteworthy that Franck, in one of his early (1956) high-temperature−high-pressure conductance explorations,[33] considered extrapolations to infinite dilution at low solvent densities from even smaller molalities ($m^{0.5} = 0.0042$) unreliable and used the Walden rule instead to estimate Λ_0. The limiting conductances calculated this way increased smoothly with decreasing density. Figure 3b also shows that below 400 $\text{kg}\cdot\text{m}^{-3}$ $\Lambda_0\eta$ decreases as the temperature decreases at constant density. These trends indicate that the size of the hydration sphere carried along by the ion increases with decreasing density, and, below 400 $\text{kg}\cdot\text{m}^{-3}$, increases as the temperature decreases. Figure 3b also shows that this increase with decreasing density is not due to any critical scaling

TABLE 2: Equivalent Conductances Λ[a]

T^b (K)	$10^6 m$ (mol·kg^{-1})	$10^6 c$ (mol·dm^{-3})	Λ (S·cm^2·mol^{-1})	δΛ (S·cm^2·mol^{-1})	T^b (K)	$10^6 m$ (mol·kg^{-1})	$10^6 c$ (mol·dm^{-3})	Λ (S·cm^2·mol^{-1})	δΛ (S·cm^2·mol^{-1})
				NaCl					
				$T = 603.28$ K; $p = 15.17$ MPa; $\rho = 650.0$ kg/m^3					
603.27	22.115	14.375	1114	0.5	603.28	610.07	396.56	1073	−0.2
603.28	22.115	14.375	1112	−1.0	603.28	1868.2	1214.7	1036	1.2
603.28	70.203	45.632	1107	0.3	603.28	5389.6	3506.2	975.1	−0.7
603.28	245.05	159.28	1092	−0.2	603.28	18107	11800	875.5	0.1
				$T = 616.23$ K; $p = 26.01$ MPa; $\rho = 650.0$ kg/m^3					
616.23	20.488	13.317	1124	−0.1	616.23	1846.7	1200.6	1045	0.5
616.23	60.229	39.151	1119	0.9	616.23	5772.4	3755.2	977.2	−0.0
616.23	174.34	113.31	1108	−0.2	616.23	18068	11772	879.3	−0.0
616.23	586.40	381.19	1084	−1.0					
				$T = 620.43$ K; $p = 17.98$ MPa; $\rho = 600.0$ kg/m^3					
620.44	16.118	9.6688	1176	−1.0	620.43	580.71	348.46	1126	0.5
620.42	17.956	10.774	1175	−1.2	620.43	1848.2	1109.7	1075	0.9
620.43	55.558	33.338	1169	0.3	620.43	5799.9	3485.7	987.4	−0.9
620.43	167.56	100.54	1156	0.1	620.43	18483	11139	865.5	0.2
620.44	371.21	222.68	1140	1.2					
				$T = 631.93$ K; $p = 26.02$ MPa; $\rho = 600.0$ kg/m^3					
631.93	20.668	12.400	1186	0.7	631.92	1940.6	1164.9	1077	0.6
631.93	61.043	36.625	1178	−0.3	631.92	5789.5	3478.	989.9	−0.3
631.93	184.83	110.89	1163	−0.5	631.92	18495	11137	864.6	0.0
631.92	602.97	361.84	1132	−0.3					
				$T = 634.89$ K; $p = 21.13$ MPa; $\rho = 550.0$ kg/m^3					
634.89	17.229	9.4766	1232	0.3	634.89	1749.5	962.97	1095	0.6
634.89	53.122	29.219	1223	0.2	634.89	5221.9	2879.6	986.9	−0.2
634.88	167.24	92.002	1204	−0.3	634.89	18478	10244	826.4	0.0
634.88	565.60	311.21	1163	−0.6					
				$T = 644.11$ K; $p = 22.70$ MPa; $\rho = 499.8$ kg/m^3					
644.11	15.152	7.5778	1273	1.0	644.12	1900.3	951.57	1067	−0.0
644.12	47.446	23.703	1261	0.6	644.11	5689.5	2859.4	927.2	0.6
644.13	167.17	83.537	1232	−0.9	644.09	18549	9417.7	756.3	−0.2
644.13	573.10	286.52	1173	−1.0					
				$T = 652.79$ K; $p = 24.81$ MPa; $\rho = 450.1$ kg/m^3					
652.79	5.7192	2.5748	1306	3.6	652.79	600.01	270.39	1141	−2.5
652.78	20.975	9.4369	1293	1.0	652.76	3247.8	1470.7	922	2.5
652.79	53.442	24.060	1275	−0.2	652.78	8386.6	3823.9	770.2	−0.6
652.78	69.270	31.225	1266	−2.9	652.75	13016	5977.2	705.2	−0.1
652.78	246.61	111.11	1214	−0.7					
				$T = 652.36$ K; $p = 23.85$ MPa; $\rho = 400.7$ kg/m^3					
652.38	3.0808	1.2335	1282	2.9	652.35	515.40	207.46	1070	1.5
652.37	10.075	4.0364	1269	−1.6	652.35	2162.7	876.05	856.4	−0.3
652.37	36.436	14.600	1248	0.0	652.36	11421	4826.9	618.8	0.0
652.36	135.09	54.23	1190	−2.5					
				$T = 652.58$ K; $p = 23.66$ MPa; $\rho = 359.3$ kg/m^3					
652.57	2.8261	1.0160	1222	−3.1	652.58	400.59	144.43	984.3	−3.9
652.58	9.8394	3.5337	1217	4.8	652.59	1829.7	671.2	759.9	3.1
652.58	30.144	10.888	1193	0.4	652.59	10700	4339.7	532.9	−0.5
652.58	101.91	36.588	1127	−0.6					
				$T = 649.59$ K; $p = 22.73$ MPa; $\rho = 323.7$ kg/m^3					
649.56	2.0783	0.67506	1052	2.7	649.59	401.11	132.93	758.4	−2.6
649.57	6.9860	2.2549	1033	−0.4	649.59	1860.5	667.46	575.9	15.0
649.57	25.521	8.2340	1012	12.0	649.63	9505.8	5140.1	490.2	−3.3
649.58	117.22	38.926	895.4	−21.0					
				$T = 652.44$ K; $p = 23.50$ MPa; $\rho = 321.4$ kg/m^3					
652.44	2.1185	0.68375	1146	6.7	652.43	400.82	131.02	803.9	3.6
652.44	5.0323	1.6275	1123	−8.0	652.42	1871.4	629.86	557.5	−8.7
652.43	22.343	7.2431	1092	−2.0	652.45	5187.4	1840.9	475.1	17.0
652.45	47.720	15.237	1058	13.0	652.43	10460	4101.9	416.0	−7.9
652.43	102.86	33.375	970.5	−13.0					
				$T = 658.08$ K; $p = 25.03$ MPa; $\rho = 320.2$ kg/m^3					
658.1	2.0479	0.65456	1245	2.2	658.08	303.94	97.676	895.9	−3.0
658.09	5.1077	1.6348	1227	−5.3	658.07	2100.1	684.59	560.7	1.0
658.09	24.918	7.9739	1185	2.5	658.07	10336	3560.8	368.5	−0.2
658.08	84.523	27.098	1087	2.8					
				$T = 652.47$ K; $p = 23.25$ MPa; $\rho = 252.3$ kg/m^3					
652.48	2.0407	0.52167	1097	−5.0	652.46	311.23	78.967	542.7	−4.7
652.5	5.2764	1.3160	1079	6.2	652.45	1779.7	462.61	319.8	9.6
652.5	23.839	5.9913	957.7	1.1	652.44	10226	2839.7	191.7	−3.0
652.47	74.517	18.701	791.0	−2.5					

TABLE 2. (Continued)

T^b (K)	10^6m (mol·kg^{-1})	10^6c (mol·dm^{-3})	Λ (S·cm^2·mol^{-1})	$\delta\Lambda$ (S·cm^2·mol^{-1})	T^b (K)	10^6m (mol·kg^{-1})	10^6c (mol·dm^{-3})	Λ (S·cm^2·mol^{-1})	$\delta\Lambda$ (S·cm^2·mol^{-1})
				$T = 658.05$ K; $p = 24.50$ MPa; $\rho = 252.2$ kg/m^3					
658.09	2.0785	0.52322	1189	−2.3	658.04	346.62	87.635	480.3	−1.7
658.08	5.9987	1.5110	1138	2.2	658.03	1960.1	501.24	258.5	1.9
658.06	22.215	5.5863	988.1	1.0	658.02	10342	2746.5	147.9	−0.5
658.05	90.343	22.836	731.6	−0.6					
				$T = 673.99$ K; $p = 27.97$ MPa; $\rho = 250.3$ kg/m^3					
673.98	2.1066	0.52801	1275	−1.6	674	355.17	88.888	391.4	−1.3
673.98	6.9064	1.7283	1159	2.1	674	1721.5	431.99	207.7	−0.4
673.99	25.283	6.3301	922.3	0.2	673.99	9457.6	2405.9	107.4	0.4
673.99	92.900	23.259	638.1	−0.0					
				$T = 652.56$ K; $p = 22.75$ MPa; $\rho = 200.0$ kg/m^3					
652.56	0.18861	0.03772	1061	−21.0	652.55	28.178	5.6389	481.9	−9.4
652.56	0.47844	0.09569	1076	25.0	652.55	104.18	20.855	293.5	−6.4
652.55	1.1422	0.22859	967.9	−25.0	652.55	464.86	93.487	157.0	−2.9
652.56	2.4086	0.48176	945.4	34.0	652.55	3051.0	618.87	70.10	−1.6
652.55	5.6597	1.1325	772.9	−6.5	652.56	8691.5	1787.9	51.05	3.2
652.56	11.668	2.3338	653.4	4.2					
				LiCl					
				$T = 603.32$ K; $p = 15.17$ MPa; $\rho = 649.8$ kg/m^3					
603.34	22.076	14.345	1076	−1.2	603.31	1835.1	1193.0	1003	0.3
603.33	59.381	38.585	1072	−0.7	603.31	5130.3	3336.9	946.2	−0.9
603.32	189.45	123.11	1060	−0.5	603.31	16760	10919	854.0	0.1
603.32	601.51	390.92	1042	2.8					
				$T = 652.75$ K; $p = 24.80$ MPa; $\rho = 450.4$ kg/m^3					
652.77	5.0481	2.2724	1285	3.3	652.75	763.47	344.41	1101	0.3
652.75	20.636	9.2934	1269	−1.5	652.75	3314.2	1501.5	903.6	0.5
652.75	76.802	34.630	1244	−1.1	652.74	13024	5982.5	696.1	−0.1
652.75	251.58	113.37	1192	−1.3					
				$T = 652.42$ K; $p = 23.50$ MPa; $\rho = 324.0$ kg/m^3					
652.41	2.1041	0.68576	1152	8.4	652.42	397.96	130.58	799.0	−9.4
652.43	7.0254	2.2528	1120	−2.0	652.42	2060.0	689.71	567.6	1.6
652.43	24.614	7.9746	1072	−19.0	652.41	10227	4011.5	458.0	−0.1
652.42	99.916	32.513	1011	20.0					
				$T = 658.07$ K; $p = 24.49$ MPa; $\rho = 251.0$ kg/m^3					
658.08	2.0872	0.52175	1164	−3.5	658.07	349.67	88.048	465.8	−0.6
658.08	6.0391	1.5160	1116	4.6	658.07	1843.8	467.75	250.7	−3.2
658.07	23.539	5.9017	953.8	−1.6	658.07	9249.8	2430.6	148.1	1.4
658.07	97.014	24.441	701.1	2.0					
				NaBr					
				$T = 603.32$ K; $p = 15.16$ MPa; $\rho = 649.8$ kg/m^3					
603.34	20.537	13.344	1100	0.7	603.31	1952.9	1269.6	1018	−0.7
603.33	62.507	40.617	1092	−1.2	603.31	5905.9	3841.6	957.2	0.1
603.32	183.59	119.30	1081	−0.5	603.3	19364	12620	867.2	−0.0
603.31	604.73	393.03	1061	1.6					
				$T = 652.65$ K; $p = 24.75$ MPa; $\rho = 450.0$ kg/m^3					
652.64	4.9484	2.2275	1314	0.2	652.65	833.01	375.57	1142	2.7
652.65	22.112	9.9526	1301	−1.2	652.65	3262.2	1475.9	963.4	−1.9
652.65	77.822	35.027	1279	−0.6	652.64	12652	5809.8	760.7	0.4
652.65	254.30	114.51	1233	0.5					
				$T = 652.45$ K; $p = 23.50$ MPa; $\rho = 322.3$ kg/m^3					
652.46	2.2207	0.71279	1154	−0.0	652.44	404.54	131.69	898.8	18.0
652.47	7.0044	2.2448	1141	−0.9	652.44	2138.1	721.08	625.6	−11.0
652.45	25.018	8.0716	1122	5.4	652.45	10452	4101.9	493.6	2.2
652.45	105.82	34.153	1018	−15.0					
				$T = 658.07$ K; $p = 24.48$ MPa; $\rho = 250.2$ kg/m^3					
658.09	2.2120	0.55135	1214	−0.3	658.06	395.48	99.281	512.6	2.9
658.08	7.1362	1.7836	1155	−1.1	658.05	1938.2	490.77	291.3	−1.4
658.08	24.909	6.2306	1022	3.5	658.05	10461	2773	175.0	0.3
658.07	106.41	26.551	753.4	−3.9					
				CsBr					
				$T = 603.32$ K; $p = 15.16$ MPa; $\rho = 649.8$ kg/m^3					
603.32	21.899	14.231	1180	−1.2	603.32	2067.9	1344.3	1096	−0.1
603.32	62.314	40.496	1174	−1.1	603.32	6548.0	4259.5	1025	−0.5
603.32	181.40	117.89	1165	0.5	603.32	20178	13150	931.7	0.1
603.32	602.18	391.36	1143	2.3					
				$T = 616.22$ K; $p = 26.00$ MPa; $\rho = 650.0$ kg/m^3					
616.22	19.475	12.658	1184	−0.8	616.22	2021.0	1314	1101	1.0
616.22	59.221	38.494	1178	−0.3	616.22	5779.3	3759.6	1036	−0.8

TABLE 2. (Continued)

T^b (K)	10^6m (mol·kg^{-1})	10^6c (mol·dm^{-3})	Λ (S·cm^2·mol^{-1})	$\delta\Lambda$ (S·cm^2·mol^{-1})	T^b (K)	10^6m (mol·kg^{-1})	10^6c (mol·dm^{-3})	Λ (S·cm^2·mol^{-1})	$\delta\Lambda$ (S·cm^2·mol^{-1})
T = 616.22 K; p = 26.00 MPa; ρ = 650.0 kg/m^3 (continued)									
616.22	182.43	118.58	1167	0.2	616.22	19768	12881	933.2	0.1
616.22	587.31	381.78	1145	0.5					
T = 620.35 K; p = 17.95 MPa; ρ = 600.1 kg/m^3									
620.36	17.933	10.762	1239	−0.6	620.35	2006.3	1205.1	1132	0.3
620.36	56.105	33.662	1232	0.0	620.35	7412.6	4458.3	1030	−0.2
620.35	176.97	106.18	1218	0.3	620.35	20828	12563	919.8	0.1
620.35	589.26	353.62	1188	0.2					
T = 631.80 K; p = 26.00 MPa; ρ = 600.3 kg/m^3									
631.84	20.619	12.376	1244	−0.1	631.79	2056.4	1235.3	1135	0.7
631.81	62.681	37.633	1236	−0.1	631.79	5815.8	3495.5	1054	−0.5
631.79	180.01	108.06	1222	−0.3	631.79	19959	12029	924.6	0.1
631.79	597.19	358.61	1193	0.2					
T = 644.19 K; p = 22.72 MPa; ρ = 499.6 kg/m^3									
644.11	14.976	7.4892	1327	1.2	644.23	1997.9	1000.1	1131	1.0
644.15	52.588	26.264	1312	−1.0	644.21	5921.1	2975.4	997.0	−0.6
644.21	172.28	86.037	1287	−0.5	644.18	20122	10221	826.0	0.1
644.23	577.51	288.63	1233	−0.2					
T = 652.75 K; p = 24.79 MPa; ρ = 450.1 kg/m^3									
652.75	5.1502	2.3180	1344	−1.9	652.75	809.18	364.76	1178	−0.5
652.75	20.243	9.1024	1335	−0.7	652.74	3089.1	1398.3	1011	−0.3
652.75	81.848	36.837	1313	2.0	652.74	13360	6140.9	790.1	0.1
652.75	256.82	115.74	1267	1.3					
T = 652.37 K; p = 23.84 MPa; ρ = 399.6 kg/m^3									
652.38	3.0676	1.2242	1315	1.5	652.36	504.55	202.51	1136	−0.5
652.36	10.015	4.0156	1305	−2.4	652.36	2342.3	949.08	930.1	−0.2
652.38	34.858	13.920	1287	−0.6	652.39	12612	5360.3	694.0	0.0
652.37	146.08	58.280	1237	2.2					
T = 652.63 K; p = 23.67 MPa; ρ = 357.7 kg/m^3									
652.63	2.9459	1.0542	1258	−2.5	652.63	404.03	146.22	1054	−1.0
652.63	9.8704	3.5287	1251	1.6	652.63	2368.3	873.32	795.0	−0.0
652.63	30.902	11.051	1227	−0.6	652.64	11994	4940.2	605.4	0.0
652.63	103.80	37.165	1177	2.6					
T = 652.47 K; p = 23.50 MPa; ρ = 319.8 kg/m^3									
652.46	2.0782	0.65955	1182	8.6	652.47	401.86	129.70	875.6	2.9
652.43	6.9641	2.2531	1165	−4.7	652.47	2122.8	708.32	619.3	−2.3
652.45	24.452	7.8682	1129	−6.5	652.5	11351	4466.5	486.3	0.5
652.47	100.38	32.171	1045	1.3					
T = 658.09 K; p = 25.06 MPa; ρ = 324.1 kg/m^3									
658.14	2.0065	0.64677	1283	3.2	658.06	310.91	101.48	997.4	−2.2
658.14	5.5329	1.7836	1269	−1.3	658.05	2177.3	721.8	671.7	3.0
658.12	21.382	6.9099	1240	0.2	658.05	11127	3915.8	466.1	−0.8
658.1	91.221	29.576	1149	−1.8					
T = 652.53 K; p = 23.25 MPa; ρ = 249.4 kg/m^3									
652.5	2.0534	0.51202	1138	−2.4	652.53	299.28	75.124	612.8	−3.7
652.54	5.3634	1.3310	1116	0.6	652.53	1902.6	484.97	350.1	−1.4
652.55	23.324	5.7768	1016	0.7	652.53	10980	3042.9	234.8	0.7
652.52	79.345	19.883	852.5	4.7					
T = 658.05 K; p = 24.48 MPa; ρ = 251.1 kg/m^3									
658.04	2.1500	0.53910	1225	−4.5	658.05	356.20	89.840	578.5	−2.2
658.04	6.0688	1.5222	1194	4.4	658.05	2127.2	539.22	315.9	−1.6
658.04	26.914	6.7784	1050	0.0	658.05	10936	2906.5	191.9	0.8
658.05	100.21	25.140	828.4	2.3					
T = 673.96 K; p = 27.97 MPa; ρ = 250.5 kg/m^3									
673.98	2.1785	0.54598	1350	−2.3	673.95	410.11	102.85	501.9	0.8
673.97	6.9322	1.7352	1277	4.1	673.95	2065.8	519.78	274.4	1.3
673.96	26.047	6.5226	1079	−1.9	673.94	10247	2617.0	153.0	−0.6
673.95	103.93	26.042	783.4	−0.9					
T = 652.53 K; p = 22.75 MPa; ρ = 200.2 kg/m^3									
652.53	1.2748	0.25536	1123	−5.1	652.53	404.31	81.111	229.2	−1.7
652.53	5.6826	1.1350	945.4	9.0	652.54	3058.9	621.00	101.6	−7.5
652.53	29.302	5.8725	617.2	1.0	652.55	14650	3078.1	83.47	4.6
652.53	97.156	19.413	398.6	−5.9					

[a] δA is the deviation of the experimental results from eq 8. [b] The temperature scale is the International Practical Temperature Scale of 1968.

effect since the decrease is even larger below the critical density of water. A critical scaling effect may be present but these results do not show it. We can get a very rough idea of the size of the hydration sphere that is carried along with the ion by calculating the Stokes' radius, that is, the radius of a spherical ion that would have this conductivity in a continuum solvent

TABLE 3: Parameters of Eq 8: Equivalent Conductances at Infinite Dilution Λ_0, Ionization Equilibrium Constants K_m, and Parameters J_2[a]

T[b] (K)	ρ_0 (kg·m^{-3})	Λ_0 (S·cm^2·mol^{-1})	10^3K_m	$-\log K_m$	$10^{-6}J_2$ dm$^{9/2}$·S·cm^2/mol$^{5/2}$	s (S·cm^2·mol^{-1})
			NaCl			
603.28	649.98	1121.3(10)	60.7(43)	1.217(32)	0.069(8)	0.8
616.23	649.99	1132.4(11)	55.8(37)	1.254(30)	0.067(8)	0.7
620.43	599.97	1185.3(11)	34.5(17)	1.462(22)	0.123(10)	1.0
631.93	599.97	1195.3(9)	31.0(10)	1.509(14)	0.117(7)	0.6
634.89	550.03	1242.5(7)	17.93(31)	1.746(7)	0.203(7)	0.5
644.11	499.81	1284.6(15)	9.34(22)	2.030(10)	0.336(21)	0.9
652.79	450.05	1311.6(30)	4.59(21)	2.338(21)	0.53(13)	2.4
652.36	400.75	1287.8(34)	2.32(10)	2.635(18)	0.28(26)	2.2
652.58	359.28	1234(6)	1.35(9)	2.869(30)	−0.5(8)	3.8
649.59	323.74	1057(25)	0.68(17)	3.17(13)	−12(8)	14.4
652.44	321.36	1148(17)	0.57(9)	3.24(8)	−9(6)	12.3
658.08	320.25	1255(6)	0.517(29)	3.286(25)	−1(2)	3.8
652.47	252.33	1128(15)	0.119(12)	3.924(45)	−27(23)	7.0
658.05	252.17	1232(5)	0.0723(20)	4.141(12)	−25(12)	2.1
673.99	250.25	1355(5)	0.0353(7)	4.452(8)	−21(21)	1.5
652.56	199.99	1106(33)	0.0094(17)	5.03(9)	−100(1400)	19.6
			LiCl			
603.32	649.85	1085.6(26)	62(11)	1.21(9)	0.067(20)	1.7
652.75	450.44	1290.0(32)	4.65(21)	2.332(21)	0.52(12)	2.0
652.42	323.98	1152(26)	0.58(14)	3.23(12)	−12(10)	15.2
658.07	251.01	1208(9)	0.0705(34)	4.152(21)	−22(22)	3.6
			NaBr			
603.32	649.84	1106.7(17)	58(6)	1.23(5)	0.053(12)	1.1
652.65	450.04	1321.6(29)	5.78(25)	2.238(20)	0.63(9)	1.8
652.45	322.3	1165(22)	0.91(20)	3.04(11)	−3(5)	13.2
658.07	250.18	1252(7)	0.0899(36)	4.046(18)	−25(14)	3.2
			CsBr			
603.32	649.85	1190.0(22)	60(7)	1.22(6)	0.061(14)	1.5
616.22	650.	1192.6(12)	61(5)	1.213(33)	0.068(8)	0.8
620.35	600.1	1248.1(6)	38.2(8)	1.418(9)	0.121(4)	0.4
631.8	600.31	1254.0(7)	36.6(10)	1.436(12)	0.123(5)	0.5
644.19	499.56	1337.9(16)	11.64(31)	1.934(12)	0.366(19)	1.0
652.75	450.06	1354.6(25)	6.25(24)	2.204(17)	0.66(7)	1.6
652.37	399.63	1322.1(28)	3.25(12)	2.488(17)	0.76(16)	1.9
652.63	357.71	1269.6(32)	1.77(7)	2.752(17)	0.16(35)	2.1
652.47	319.82	1187(10)	0.76(8)	3.12(5)	−5.3(27)	6.2
658.09	324.08	1291(4)	0.816(34)	3.088(18)	−0.3(10)	2.7
652.53	249.37	1165(7)	0.149(7)	3.828(20)	−27(9)	3.3
658.05	251.11	1260(7)	0.116(5)	3.936(20)	−9(11)	3.6
673.96	250.49	1402(7)	0.0668(21)	4.175(14)	−9(16)	2.7
652.53	200.21	1229(28)	0.0137(15)	4.86(5)	−518(370)	7.4

[a] The densities, ρ_0, calculated from the Hill equation of state[28], correspond to the median pressures from Table 2. s is the standard deviation of the experimental Λ_0 values from eq 8. The numbers in parentheses are the uncertainties of the last digit. [b] The temperature scale is the International Practical Temperature Scale of 1968.

with the same viscosity. The Stokes' radius is inversely proportional to $\Lambda_0\eta$ and varies from about 0.2 nm at the highest densities to a maximum of 0.4−0.5 nm at the lowest densities. Why do ions, on average, carry more water molecules along with them at the lower densities? Figure 4 suggests two effects that could contribute to the increasing Stokes' radius at low densities. This figure shows the plots of the pair correlation function, g_2, from Monte Carlo simulations of models for a chloride ion in water at two widely different bulk densities, ρ^*, near the critical temperature. At a given radius and lower ρ^* the density of water, $\rho = \rho^* g_2$, is much lower and g_2 is much higher.[34] As a result of the lower density at all distances, the dielectric constant is much lower, and the electrostatic forces due to the ion are much higher. Figure 4 shows that at $R =$ 0.7 nm $g_2[\rho^* = 10$ kg·m$^{-3}]$ is almost twice $g_2[\rho^* = 320$ kg·m$^{-3}]$. As a result of the higher g_2 at 0.7 nm when $\rho^* = 10$ kg·m^{-3} the density ρ is much larger than ρ^* and the viscosity is much larger than the bulk viscosity. Consequently, more water molecules should move with the ion. The same effect, although less dramatic, should operate even for smaller changes in the bulk density. Recent experimental[35] and theoretical[36] evidence indicates a similar effect for attractive nonpolar solutes near a nonpolar solvent critical point since the maximum in the solute "local density" (which reflects short range order) occurs at densities well below the critical density. The above discussion is of course oversimplified. A quantitative model for dielectric friction and electrostriction is needed since both of these effects are very important near the critical point.

Now let us turn to a discussion of the effects of the size of the ion on the limiting equivalent conductance. Although the differences in conductance are not much larger than the experimental errors, we can get estimates of the differences by comparing measurements made at nearly the same temperatures and pressures (see Table 3) ignoring the small differences. Fitting the differences to polynomials in temperature and density we found that the best representation of the data is

$$\Lambda_0[\mathrm{MX}] - \Lambda_0[\mathrm{NaCl}] = a + b(\rho_0 - 400\ \mathrm{kg\cdot m^{-3}}) \quad (12)$$

with values of a and b given in Table 4. The differences have the same sign as the differences at 25 °C and 1 bar and are somewhat larger (see Table 4). Apparently similar effects are

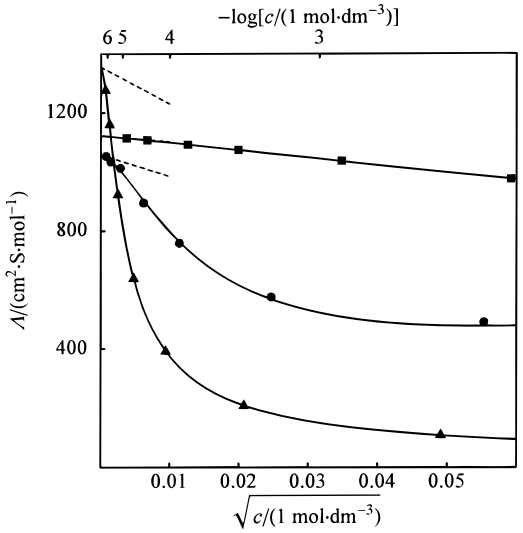

Figure 2. Equivalent conductance as a function of concentration for NaCl(aq): experimental results (symbols), corresponding calculation from eqs 8−11 (continuous lines), and corresponding Debye−Hückel−Onsager slopes (broken lines). The symbols represent the experimental results at (■) $\rho_0 = 650$ kg·m^{-3}, $T = 603.3$ K; (●) $\rho_0 = 324$ kg·m^{-3}, $T = 649.6$ K; (▲) $\rho_0 = 250$ kg·m^{-3} , $T = 673.9$ K.

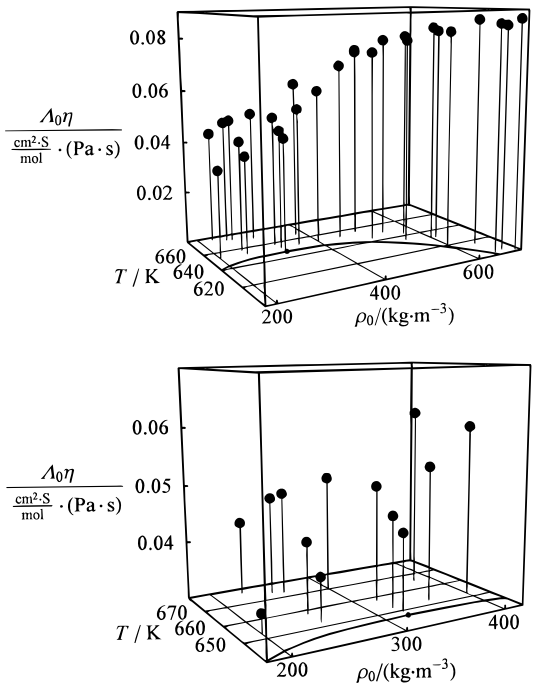

Figure 3. Values of $\Lambda_0\eta$, where η is the viscosity of pure water, calculated from equation of Watson *et al.*[26] plotted as a function of density and temperature: (a, top) all of results (b, bottom) results below 400 kg·m^{-3} showing the decrease with decreasing temperature at constant density. The curved line is the boundary of the two-phase region for water with the black dot indicating the critical point.

operative at high temperatures as at room temperature. The smaller ions polarize the water more and so increase the strength of the water−water hydrogen bonds between the first and second hydration spheres.

The association constants for NaCl were correlated as a function of density and temperature using the following empirical form,[37]

$$-\log K_m = a_1 - \frac{1200\ \mathrm{K}}{T} + a_2\rho + \frac{a_3}{\rho} + a_4 \exp[a_5(T - T_c) + a_6\rho^3] \quad (13)$$

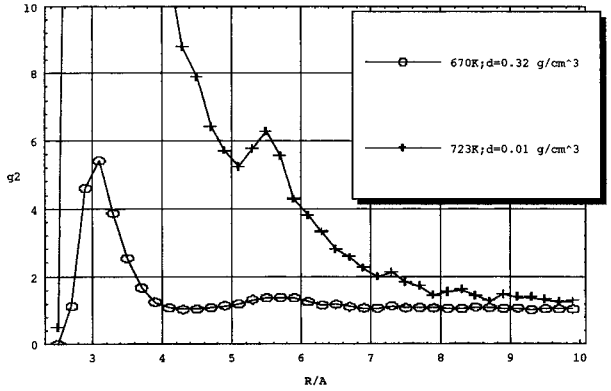

Figure 4. Plot of the ion−water pair correlation function, g_2, calculated from a Monte Carlo simulation of a model chloride ion in water as a function of distance from the ion. See Wood *et al.*[34] for details of the simulation.

TABLE 4: Differences in Λ_0 for Various Salts. Values of *a* and *b* in Eq 12

MX	a^a	b^a	$\langle\delta/\sigma\rangle^b$	$\Delta\Lambda_0$[298 K]^c
LiCl	−25 (4)^d	−0.05(2)	1.1	−11.4
NaBr	6 (10)	−0.06(5)	1.7	1.8
CsBr	41 (6)	−0.09(3)	1.5	29.0

^{a} Units are S·cm^2·mol^{-1} for ρ_0 in kg·m^{-3}. ^{b} Average value of $[\Delta\Lambda_0(\mathrm{expt}) - \Delta\Lambda_0(\mathrm{calc})]/\sigma$. ^{c} Λ_0[MX] − Λ_0[NaCl] at 298.15 K and 1 bar. ^{d} Numbers in parentheses are the 95% confidence limits of the last digit as obtained from the weighted fit to eq 12.

with the coefficients $a_1 = 1.5089$, $a_2 = -0.000\,435\,83$ (kg·m^{-3})$^{-1}$, $a_3 = 1291.0$ kg·m^{-3}, $a_4 = -1.7768$, $a_5 = -0.037\,829$ K^{-1}, $a_6 = -4.417 \times 10^{-8}$ (kg·m^{-3})$^{-3}$. It can be expected that if eq 13 was used to analyze the experimental volumetric data from Majer and Wood,[21] the resulting volumes at infinite dilution (expressed here by eq 6) would be somewhat different, but this should result in very small changes in Λ_0 and K_m.

Equation 13 essentially agrees with the results for NaCl obtained by others[6,7,38] at high temperatures, where we assumed a linear dependence of pK_m on $1/T$, and it should give reasonable results at temperatures much higher than 674 K, the upper limit of this work. However, it is valid only in the density range 200 − 700 kg·m^{-3} and should not be used for extrapolation to low steam densities. For example, for saturated vapor from 200 to 85 kg·m^{-3} eq 13 gives equilibrium constants corresponding to significantly less ion pairing than the experimental results of Lukashov *et al.*,[4] and the difference increases with decreasing density.

Figure 5 shows a comparison of the logarithms of the equilibrium constants for the ion pair dissociation reaction (eq 4) of NaCl, both measured and calculated from eq 13, with experimental results of Fogo *et al.*[2] and Pearson *et al.*[3] recalculated using the FHFP equation. The values of pK_m show no critical anomaly, although at densities lower than the critical density there is a decrease in pK_m as temperature decreases from supercritical values. The results of Fogo suggested this change of slope and it is confirmed by the present results. Good agreement with Fogo's results is obtained, particularly in the intermediate density region, as shown more precisely in Figure 6, where deviations of several sets of experimental pK_m results from eq 13 are plotted in as a function of water density. The agreement with Fogo *et al.*[2] and Pearson *et al.*[3] results is remarkable considering that these results were obtained over 40 years ago.

Equation 13 cannot, of course, predict pK_m of NaCl at the critical point, but the value it gives at $T = 647.13$ K and $\rho_0 =$

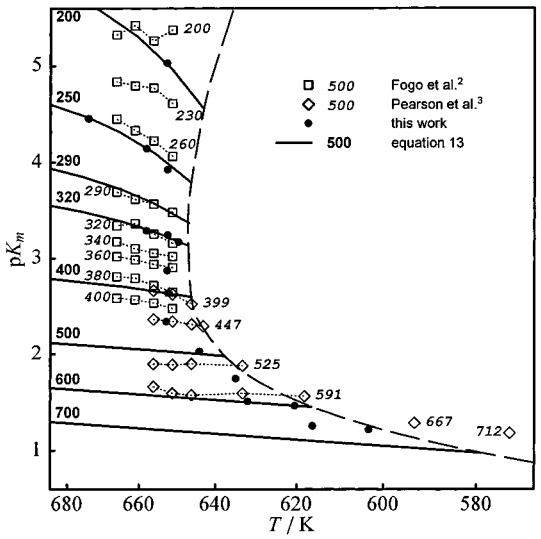

Figure 5. pK_m for NaCl(aq) as a function of temperature and density. The symbols represent experimental results and the continuous lines are calculated from eq 13. The dotted lines connect series of experimental points at the same solvent densities. The numbers, with their representative examples shown in the legend, are densities in kg·m^{-3}, corresponding to either symbols or lines. The broken line is the two-phase region envelope. Symbol assignments are the same as in Figure 1. The results of Fogo *et al.*[2] were recalculated using the FHFP equation. The *x* axis is linear with respect to 1/*T*.

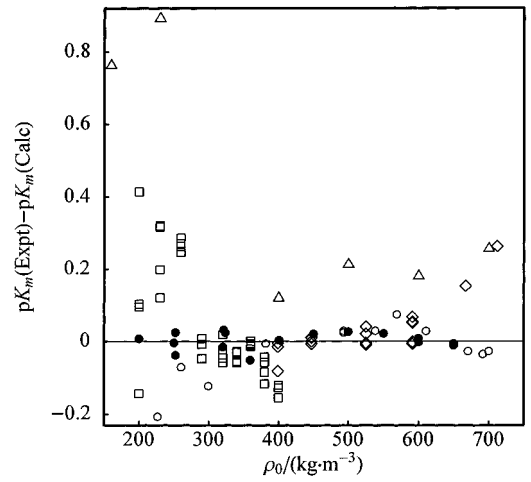

Figure 6. Deviations of experimental results for NaCl(aq) from eq 13, [pK_m(expt) − pK_m(calc)], as a function of water density. Symbol assignments are the same as in Figure 1.

322 kg·m^{-3} is 3.12, only slightly less than 3.37 obtained by Marshall[39] from conductance measurements at conditions far removed from the critical region. The correlation[1] used by us previously, and based on measurements done mostly on the 28 MPa isobar, yielded $pK_m = 3.33$ at these conditions, and this is again close to the Marshall's value. The equation given by Ho *et al.*[7] gives $pK_m = 3.14$ at the critical point (extrapolated from experimental data above 673 K), very close to the value obtained from eq 13. At temperatures higher than 673 K and at densities 400−500 kg·m^{-3} eq 13 is in good agreement with the pK_m values of Ho *et al.*,[7] Quist and Marshall,[6] and Franck.[38] We believe that at densities higher than 500 kg·m^{-3} each of these three sources gives pK_m values that are too low, with the results of Ho *et al.*[7] being the closest to the present results. For example, at 700 kg·m^{-3} and 823 K, the differences in pK_m between eq 13 and refs 7, 6, and 38 are (0.23, 0.51, and 0.60) log units, respectively. At 300 kg·m^{-3} the differences are even larger; however, due to a considerable curvature of $pK_m(T)$ it is not possible to estimate pK_m at this density and at high temperatures with an accuracy better than at most ±0.5 log units using all the available experimental data. The error of eq 13 is estimated to be between ±0.1 log units at 700 kg·m^{-3} and ±0.5 log units at 300 kg·m^{-3}

TABLE 5: Differences in pK_m for Various Salts. Values of *c* and *d* in Eq 14

MX	*c*	*d*	$\langle\delta/\sigma\rangle$[a]
LiCl	*b*	0.0003 (1)	1.33
NaBr	−0.08 (3)[c]	0.0005 (2)	0.92
CsBr	−0.15 (2)	0.0006 (1)	0.97

[a] Average value of [ΔpK_m(expt) − ΔpK_m(calc)]/σ. [b] The coefficient was not significant at the 90% confidence limit. [c] Numbers in parentheses are the 95% confidence limits of the last digit as obtained from the weighted fit to eq 14.

The preceding discussion refers to NaCl(aq), which has been measured the most extensively. As before, we can get estimates of pK_m[MX] − pK_m[NaCl] by comparing measurements made for MX with the correlation for NaCl, eq 13. Fitting the differences to the equation

$$pK[\mathrm{MX}] - pK[\mathrm{NaCl}] = c + d(\rho_0 - 400\ \mathrm{kg\cdot m^{-3}}) \qquad (14)$$

gave the coefficients reported in Table 5.

Ion pairing (and pK_m) increases in the sequence CsBr < NaBr < NaCl ≈ LiCl. This is consistent with our previous results, and additionally for the pair NaCl and NaBr with the conclusions of Marshall and his co-workers.[40,41] The difference between LiCl(aq) and NaCl(aq) is not statistically significant, and it is not in agreement with the trend favoring dissociation of the pairs of larger ions. There are few literature data on ionization equilibrium in LiCl(aq) at high temperatures,[38,42] and their accuracy is not sufficient to show any small differences. However, a reversal in the ordering of the apparent volumes of these two solutes (which were quite close to each other) was discussed by Majer and Wood.[21] The subtle relationships between the ability to form ion pairs by ions of different sizes at different thermodynamic conditions are a result of competition between solvent molecules and ions to occupy the space in close proximity of an ion. In dilute solutions, where the solvent is abundant, the sizes of different hydrated ions are relatively close to each other. The differences between their properties are relatively small, and they may depend on second order considerations, like, for example, the particular number and configuration of the water molecules in the first hydration spheres of the cations or anions.

Acknowledgment. The authors thank Anneke Levelt-Sengers for her helpful comments on the critical effects and Josef Sedlbauer for help with fitting eq 14 to the experimental data. Research sponsored by the National Science Foundation under Grant 9416564 and by the Division of Chemical Sciences, Office of Basic Energy Sciences, U.S. Department of Energy, under contract DE-AC05-96OR22464 with Oak Ridge National Laboratory, managed by Lockheed Martin Energy Research Corp.

References and Notes

(1) Zimmerman, G., H.; Gruszkiewicz, M. S.; Wood, R. H. *J. Phys. Chem.* **1995**, *99*, 11612.
(2) Fogo, J. K.; Benson, S. W.; Copeland, C. S. *J. Phys. Chem.* **1954**, *22*, 765.
(3) Pearson, D.; Copeland, C. S., Benson, S. W. *J. Phys. Chem.* **1963**, *85*, 1044.
(4) Lukashov, Yu. M.; Komissarov, K. B.; Gobubev, B. P.; Smirnov, S. N.; Svistunov, E. P. *Thermal Eng.* **1976**, *22*, 89.
(5) Martynova, O. I.; Belova, Z. S; Golubev, B. P.; Samoilov, Yu. F. *Thermal Energy* **1965**, *12*, 91.
(6) Quist, A. S.; Marshall, W. L. *J. Phys. Chem.* **1968**, *72*, 684.

(7) Ho, P. C.; Palmer, D. A.; Mesmer, R. E. *J. Solution. Chem.* **1994**, *23*, 997.
(8) Justice, J. C. In *Comprehensive Treatise of Electrochemistry;* Conway, B. E., Bockris, J. O'M., Yeager, E., Ed.; Plenum Press: New York, 1983, Vol. 5, p 310.
(9) Barthel, J.; Feuerlein, F.; Neuder, R.; Wachter, R. *J. Solution. Chem.* **1980**, *9*, 209.
(10) Fisher, F. H.; Fox, A. P. *J. Solution. Chem.* **1979**, *8*, 627.
(11) Zimmerman, G. H. Ph.D. Dissertation, University of Delaware, January 1994.
(12) Chiu, Y-C; Fuoss, R. M. *J. Phys. Chem.* **1968**, *72*, 4123.
(13) Gunning, H. E.; Gordon, A. R. *J. Chem. Phys.* **1942**, *10*, 126.
(14) Shedlovsky, T.; Brown, A. S.; MacInnes, D. A. *Trans. Electrochem. Soc.* **1934**, *66*, 165.
(15) Majer, V.; Gates, J. A.; Inglese, A.; Wood, R. H. *J. Chem. Thermodyn.* **1988**, *20*, 949.
(16) Majer, V.; Inglese, A.; Wood, R. H. *J. Chem. Thermodyn.* **1989**, *21*, 321.
(17) Majer, V.; Inglese, A.; Wood, R. H. *J. Chem. Thermodyn.* **1989**, *21*, 397.
(18) Majer, V.; Hui, L.; Crovetto, R.; Wood, R. H. *J. Chem. Thermodyn.* **1991**, *23*, 213.
(19) Majer, V.; Crovetto, R.; Wood, R. H. *J. Chem. Thermodyn.* **1991**, *23*, 333.
(20) Majer, V.; Hui, L.; Crovetto, R.; Wood, R. H. *J. Chem. Thermodyn.* **1991**, *23*, 365.
(21) Majer, V.; Wood, R. H. *J. Chem. Thermodyn.* **1994**, *26*, 1143.
(22) Pitzer, K. S. In *Activity Coefficients in Electrolyte Solutions*, 2nd ed.; Pitzer, K. S., Ed.; CRC Press: Boca Raton, FL, 1991.
(23) O'Connell, J. P.; Sharygin, A. V.; Wood, R. H. *Ind. Eng. Chem. Res.*, in press.
(24) Marshall, W. L. *J. Phys. Chem.* **1970**, *74*, 346.
(25) Fernandez-Prini, R. *Trans.Faraday Soc.* **1969**, *65*, 3311.
(26) Watson, J. T. R.; Basu, R. S.; Sengers, J. V. *J. Phys. Chem. Ref. Data* **1980**, *9*, 1255.
(27) Archer, D. G.; Wang, P. *J. Phys. Chem. Ref. Data* **1990**, *19*, 371.
(28) Hill, P. G. *J. Phys. Chem. Ref. Data* **1990**, *19*, 1233.
(29) Chang, R. F.; Levelt-Sengers, J. M. H. *J. Phys. Chem.* **1986**, *90*, 5921.
(30) Quist, A. S.; Franck, E. U.; Jolley, H. R.; Marshall, W. L. *J. Phys. Chem.* **1963**, 67, 2453.
(31) Quist, A. S.; Marshall, W. L. *J. Phys. Chem.* **1965**, *69*, 2984.
(32) Marshall, W. L *J. Chem. Phys.* **1987**, *87*, 3639.
(33) Franck, E. U. *Z. Phys. Chem. (Frankfurt)* **1956**, *8*, 107.
(34) Wood, R. H.; Carter, R. W.; Quint, J. R.; Majer, V.; Thompson, P. T.; Boccio, J. R. *J. Chem. Thermodyn.* **1994**, *26*, 225.
(35) Carlier, C.; Randolph T. W. *AICHE J.* **1993**, *39*, 876.
(36) Chialvo, A. A.; Cummings, P. T. *AICHE J.* **1994**, *40*, 1558.
(37) Note that the coefficient of T^{-1} in this equation is −1200 K, the same as in eq 6 in Zimmerman et al.,[1] which contains a printing error.
(38) Franck, E. U. *Angew. Chem.* **1961**, 73, 309.
(39) Marshall, W. L. *J. Chem. Soc., Faraday Trans.* **1990**, *86*, 1807.
(40) Quist, A. S.; Marshall, W. L. *J. Phys. Chem.* **1968**, *72*, 2100.
(41) Dunn, A. D.; Marshall, W. L. *J. Phys. Chem.* **1969**, *73*, 723.
(42) Mangold, K.; Franck, E. U. *Ber. Bunsenges. Phys. Chem.* **1969**, *73*, 21.